SPECTRAL OBSERVATIONS OF GEOSTATIONARY SATELLITES

Serebryanskiy A.V.[1], Omarov Ch.T.[1], Aimanova G.K.[1], Krugov M.A.[1], Akniyazov Ch.B.[1,2]

[1]Fesenkov Astrophysical Institute, Almaty, Kazakhstan, akniyazov@aphi.kz
[2]al-Farabi Kazakh National University, Almaty, Kazakhstan

One of the main tasks of the situational awareness system in near-Earth space is to determine the type and class of observed objects by analyzing its reflection spectra. This paper proposes a methodology and interpretation of the spectral observational data of geostationary orbit satellites obtained at the Tian Shan Astronomical Observatory (Kazakhstan) from June-December 2021. 8 geostationary objects, the type and design features of which are known were selected as observation targets. The selected satellites are stable (no fast rotation of these objects was detected) and have large reflecting surface areas. An analysis of the obtained reflection spectra shows the dependence on the phase angle of the object. The studies carried out are especially relevant for objects in high orbits, where the only currently available methods of detection and study are ground-based optical photometry and spectroscopy using meter-class telescopes.

Keywords: Optical measurements, geosynchronous Earth orbit, spectroscopy, artificial Earth satellites, orbital mechanics, observations, material spectra.

Introduction

Despite the rapid development of satellite fleets in low orbit (LEO), the geosynchronous orbit (GSO) band remains one of the most sought-after resources in near-Earth space, used by most commercial telecommunications and military satellites, each of which can cost several hundred million dollars.

One of the main tasks of the situational awareness system in near-Earth space is to determine the type and class of observed objects. One of the methods for obtaining these characteristics is the analysis of reflection spectra. This task is especially relevant for objects in high orbits, where the only methods of detection and research currently available are ground-based optical photometry and spectroscopy using meter-class telescopes (as the most effective tool, given their prevalence, availability, operating costs, etc.). Spectroscopy methods have a number of advantages over traditional multicolor photometry, since, in addition to much more information contained in the spectra, it allows one to obtain object brightness estimates simultaneously in all spectral bands, which is very important for objects in the geostationary zone [1,3,15]. Most of the objects in the GEO zone are fragments of space debris (uncontrolled objects of artificial origin), which include upper stages, parts of the fragmentation of the spacecraft, uncontrolled satellites, etc., often showing a rapid change in brightness (due to proper rotation). The rate of such a change can be from fractions of a second to minutes. It becomes clear that it is not possible to determine the color index (as one of the main indicators of the optical characteristics of the reflective surface) from the brightness values in different filters obtained by the traditional method of multicolor photometry. In addition, as shown in [2,11,12], different materials used in the space industry exhibit a variety of changes due to the effects of outer space conditions, which leads to unique spectral characteristics of each of the materials. This, in turn, also makes it possible to identify the object and determine its state.

The method of reflection spectroscopy has a number of complexities, the main of which is the inability to study small-sized objects with low brightness. However, this difficulty can be solved by using an efficient low-resolution spectrograph equipped with EMCCD in combination with a large aperture instrument, which is the AZT-20 telescope of the Assy-Turgen observatory. Such a spectrograph was developed and installed at AZT-20 at the end of 2021, and it is planned to be operational from 2022. To refine the methodology for analyzing reflectance spectra, selecting the initial class of objects of study, and developing the methodology for obtaining and preprocessing CCD spectral observation data, it was decided to conduct a series of observations of selected GSS using the Zeiss-1000 "West" telescope of the Tian Shan Observatory (TShAO), using low-resolution slit spectrograph.

1 Observations

The GSO objects with a known type, design features, stable (no fast rotation of these objects was detected), having large reflective surfaces, which is, the brightness of objects in the V-band is not higher than magnitude 11 were selected as observational targets. Another criterion was the observational visibility of these objects at the TShAO observatory. A list of these objects is shown in Table 1.

Table 1. List of objects selected for observations.

NORAD ID	Shape	Mean cross-sectional area, m^2
30793	Box + 2 Pan	13.8
32404	Box + 1 Dish + 2 Pan	458.1
38098	Box + 2 Pan	56.1
39460	Box + 2 Pan	22.2
28899	Box + 1 Dish + 2 Pan	57.2
39728	Box + 2 Pan	17.0
37749	Box + 2 Pan	10.7
29230	Box + 2 Pan	15.9

A series of five spectroscopic observations of satellites of the KazSat constellation and several GSSs were carried out using the low-resolution spectrograph of the Zeiss-1000 "Western" telescope of the TShAO. The spectrograph is equipped with a diffraction grating of 300 lines/mm, and a SBIG STT 3200 CCD camera with a size of 2184✕1472 pixels (pixel size 6.8 μm) as a detector was used, which made it possible to obtain spectra in the wavelength range from ~4000 Å to ~ 8000 Å, with a dispersion of about 3Å. To obtain the optimal signal-to-noise ratio, the mode of averaging the signal over 2✕2 pixels (2nd binning) was used, and the exposure time for different objects was chosen in the range from 60 seconds to 1800 seconds. The observations were carried out on the following nights: June 29, November 6, 24, 30 and December 1, 2021.

1.1 Preliminary data reduction

Data preprocessing was performed using standard procedures utilizing the Image Reduction and Analysis Facility (IRAF) package which includes dark frame subtraction, cosmic ray removal, and wavelength calibration. An example of the reduced spectra is shown in Fig.1.
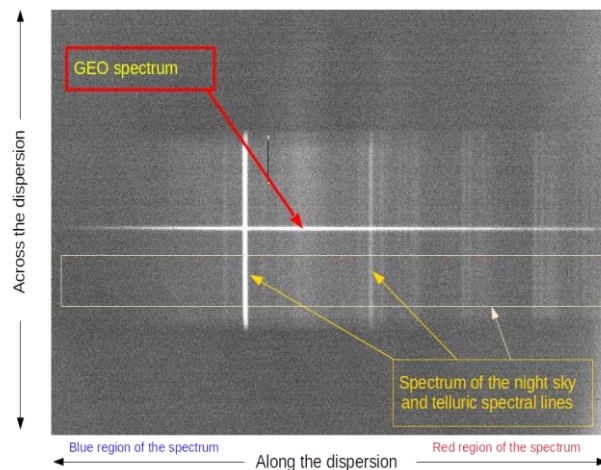

Fig. 1. An example of a CCD frame of the GSS spectrum obtained on the Zeiss-1000 "Western" slit spectrograph of TShAO. Range from ~4500Å to 7600Å

For wavelength calibration, after each spectrum of the GSO object, the spectra of a standard source - a He-Ne-Ar lamp - were obtained. Preprocessing is identical for both the GSS spectra and the spectra of standard stars. To take into account the effect of changes in the air mass during observations, the effect of flux absorption in each wavelength range (extinction) was taken into account. The resulting GSS reflectance spectra were obtained by dividing the GSS spectrum by the spectrum of the standard star.

1.2 Reference stars selection

For the task of analyzing the reflection spectra of the GSS, it is important to choose standard stars whose spectral type is as close as possible to the solar one. Additional criteria are available for observations on a given night, as well as sufficient brightness of the star to obtain a spectrum with a high signal-to-noise ratio. The list of standard stars selected according to these criteria is given in Table 2.

Table 2. List of selected standard stars

Standard star	RA	DEC	Sp type	V mag
HD 14754/HIP 11106	$02^h22^m56^s.65$	+08°32'43''.65	F0	7.6
HD 11532	$01^h53^m18^s.37$	+00°22'23''.28	G8III/IV	9.7
HD 292561	$06^h51^m33^s.73$	-00°11'31''.52	G2V-G3V	10.7
HIP 111063/HD 213199	$22^h29^m58^s.797$	-16°28'07''.395	G2V C	8.19
HIP 118115/HD 224383	$23^h57^m33.518$	-09°38'51''.070	G3V C	7.88
TYCHO 4893-1379/HIP 46404/HD 81809	$09^h27^m46^s.808$	-06°04'17''.008	G1.5IV-V C	5.42
TYCHO 5338-724/HIP 23831/HD 33093	$05^h07^m24^s.963$	-12°29'28''.572	G0IV C	5.97

2 Methodology of spectral data analysis

2.1 Reflectance spectra

Reflectance spectroscopy is a powerful characterization tool that helps with the identification of micrometeoroid and orbital debris material (collectively referred to by space agencies as MMOD - Micrometeoroid and orbital debris), especially in the research related to asteroids since the 1970s. In the 1990s, its application expanded to the characterization of materials for orbiting spacecraft [4,13,14]. Ground-based spectral measurements are valuable references that assist remote optical observations in analyzing the composition of space debris material, object position and orbital motion. Reflectance spectroscopy has proven to be a viable tool for providing the aerospace industry with detailed data on the characteristics of materials commonly used in spacecraft construction, such as iridium aluminum, stainless steel, glass, gold, various silicone paints, and different types of solar cells [5]. Spectroscopic measurements taken on pieces of spacecraft materials in the lab can then be compared with spectroscopic or photometric data from orbital debris taken remotely with telescoping instruments. Research data are stored in the National Aeronautics and Space Administration (NASA) Johnson Space Center Spectral Database [6].

In the practice of spectral studies, an approximate, but a simpler and more convenient method for obtaining reflection spectra is widely used, which does not require registration of the spectral distribution of energy in the solar radiation spectrum at the time of observation. At the same time, despite the obvious advantages, such a simplified method also has significant disadvantages, most often associated with the low quality of the resulting reflection spectrum, i.e. the noise. If at the stage of recording the spectrum of an object, a reduction in the level of statistical noise can be achieved by simply increasing the exposure time, then the following procedure for dividing the spectral data series to obtain a reflection spectrum introduces an additional noise component into the final result. The most significant source of the additional noise component in the reflection spectra is the solar analog stars themselves.
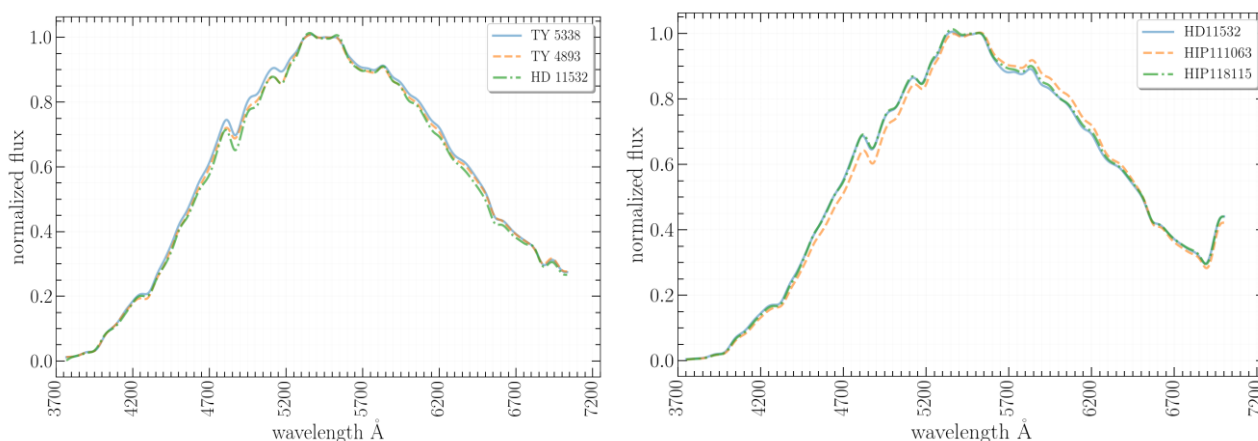
Fig. 2. Standard spectra: on the left - TYCHO 4893-1379 (HD 81809), TYCHO 5338-724 (HD 33093) and HD 11532 as of December 1, 2021; right - HD 11532, HIP 111063 and HIP 118115 as observed on November 29, 2021.

At least two solar analogue stars from Table 2 were observed every night. Examples of the spectra of the standard stars obtained on two different nights are shown in Fig.2. As a rule, we calculated the reflectance spectrum of each object with each standard by dividing its flux by the flux of the solar analog star observed on the same night in the most similar air mass conditions.

2.2 Smoothing reflectance spectra

A careful search for "ideal" standard stars, which can be considered good spectral analogues of the Sun [7,8,9], has so far only led to a list of about a dozen stars (magnitudes in the range 4^m - 6^m and spectral type G0V - G3V). Therefore, the search for methods for minimizing additional noise in the spectra is of current interest. A fairly effective way to suppress noise in the reflection spectra is their smoothing.

To smooth the reflection spectra, we used a Butterworth filter. The feature of this filter is to effectively remove unwanted noise from the data in the high-frequency range, while not affecting the data in the low-frequency region. In other words, the frequency response of this filter is constant over the passband and drops to zero in the frequency range we deem to be noise.

The Butterworth filter was implemented in the *scipy* package [10] by the *signal.butter* method, which took the filtering degree and the cutoff frequency in units of the Nyquist frequency as parameters. In our case, the filtering degree was set to 3, and the cutoff frequency was 0.055, which corresponds to smoothing the spectrum in a window of about 100Å band with a spectral resolution of about 3Å. Testing with various cutoff frequencies showed that this was the optimal value and the smoothing result, when this parameter was chosen in a reasonable range around 0.055, did not change the conclusions.

The smoothing process itself was carried out by the *signal.filtfilt* method of the *scipy* package. The results of the smoothing process are illustrated in Fig. 3-6.

In each panel of the figure, top part, the observations of the geostationary satellite spectra obtained at different phase angles are shown, below - the reflection spectra obtained for these phase angles. Reflection spectra are normalized to a wavelength of 0.55 *μm*. The NORAD ID number, the year of launch and the device owner country are written in the bottom line.
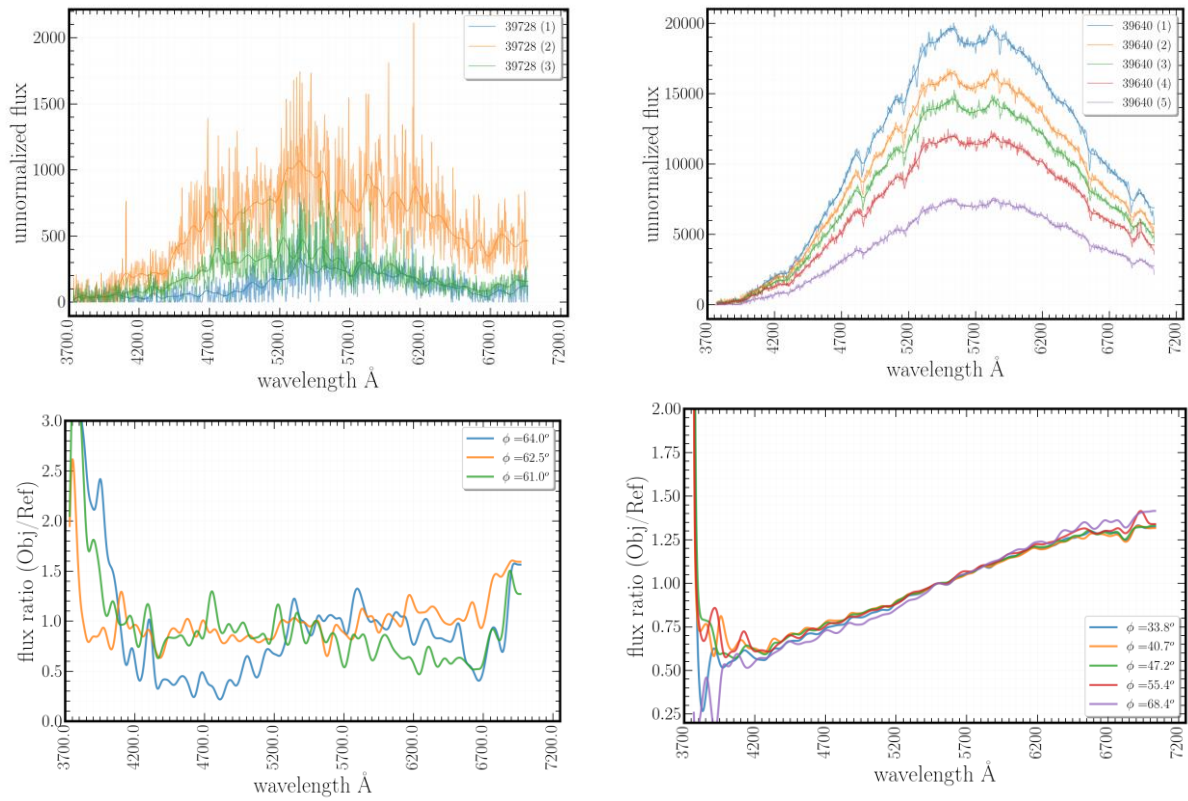
Fig. 3. Reflective spectra of GSS launched between 2013-2014 with different phase angles □. The left column shows 39728 and the right column shows 39640 with unnormalized flux (top) and normalized (bottom).

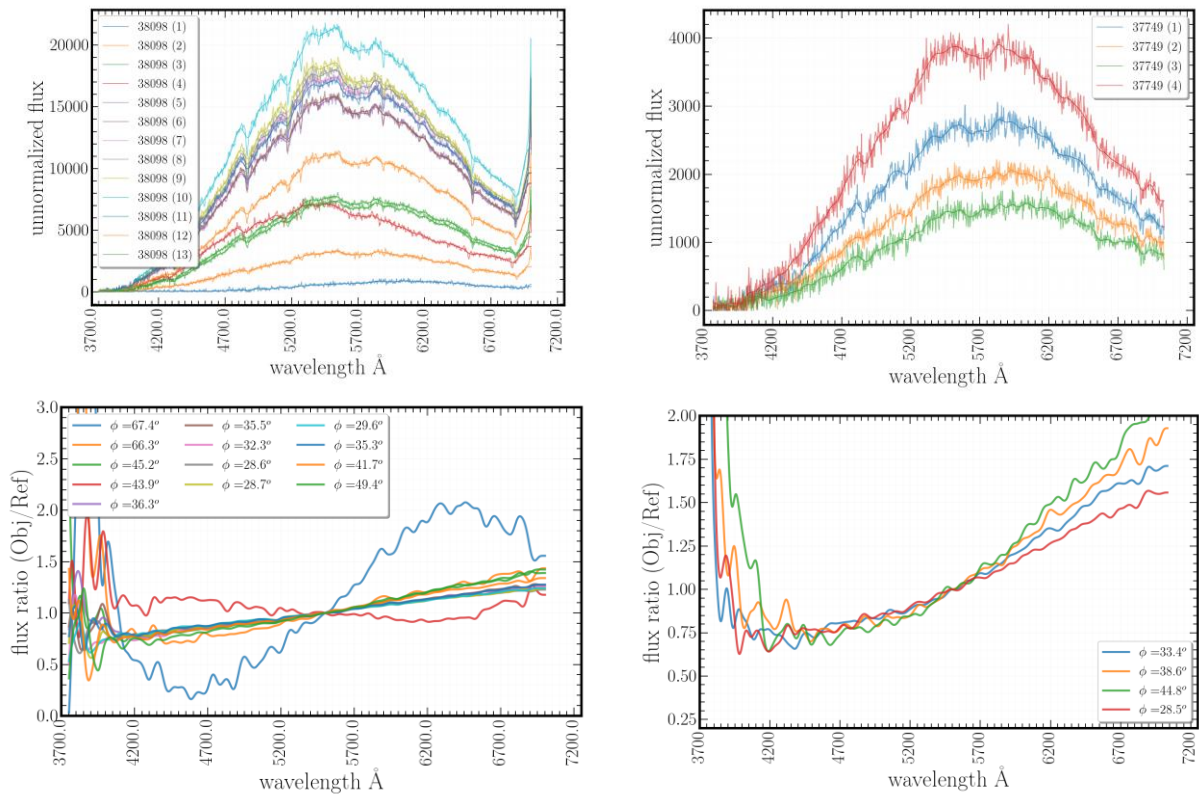**Fig. 4**. Reflective spectra of GSS launched between 2011-2012 with different phase angles □. The left column shows 38098 and the right column shows 37749 with unnormalized flux (top) and normalized (bottom).
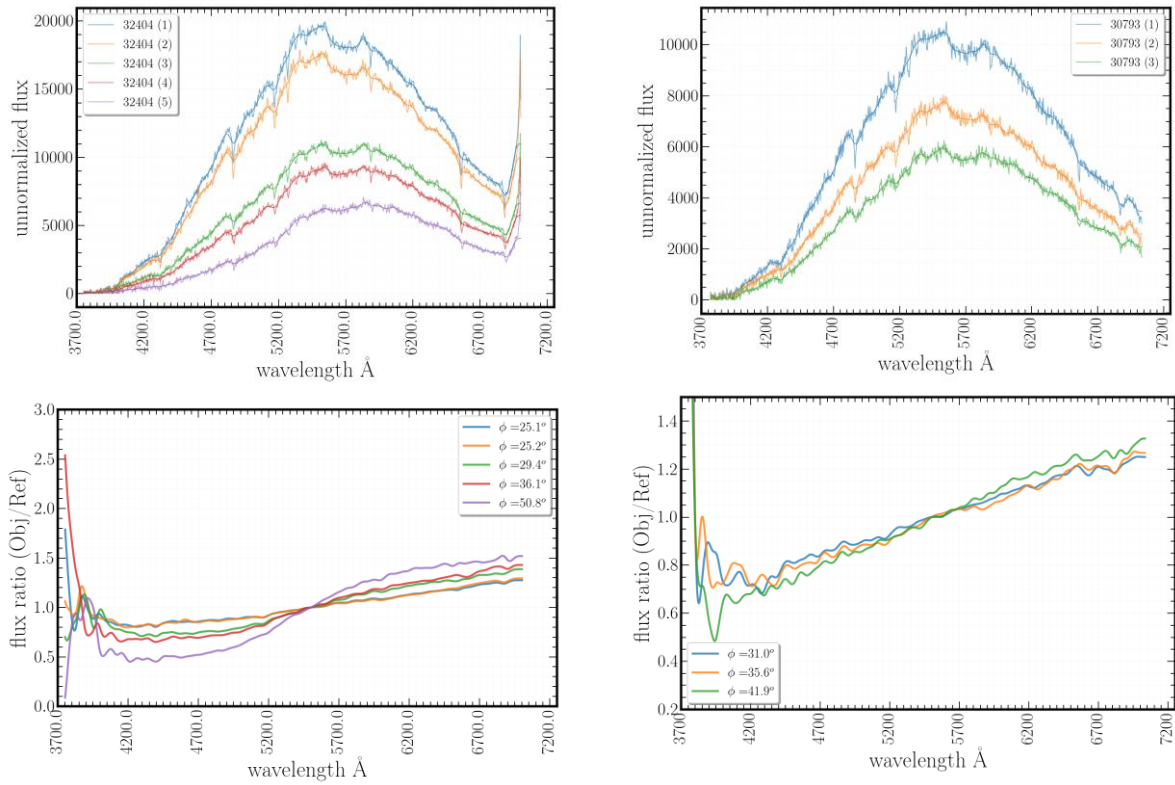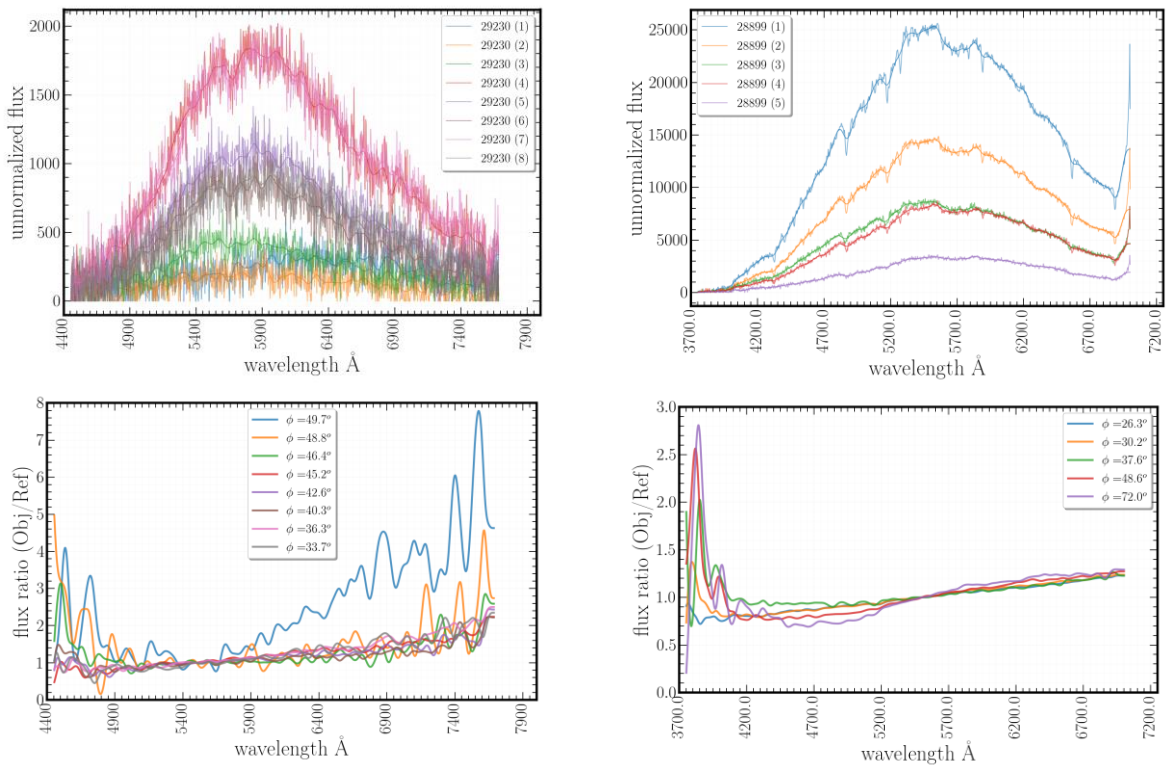
Fig. 5. Reflective spectra of GSS launched between 2007-2008 with different phase angles ⬜. The left column shows 32404 and the right column shows 30793 with unnormalized flux (top) and normalized (bottom).

Fig. 6. Reflective spectra of GSS launched between 2005-2006 with different phase angles ⬜. The left column shows 29230 and the right column shows 28899 with unnormalized flux (top) and normalized (bottom).

3 Discussion

It can be seen from Fig. 2 that the normalized fluxes of the selected solar analog standard stars show a good match. The resulting reflectance spectra were calculated using different standard stars observed on the same night as the object turned out to be identical in many cases along the course of change.

There is a dependence on the phase angle of the object, but at this stage, due to the limited observational material, it is impossible to trace the dependence of changes in the reflection spectrum on the lifetime of the device in orbit.

As a parameter for analyzing the change in the reflection spectrum depending on the phase angle, we have chosen the slope factor (α) of the reflection spectrum (hereinafter referred to as the "spectrum slope"), which is determined from the linear approximation of the reflection spectrum as a function of the wavelength: $flux_{fit} = \alpha \times \lambda + \beta$.

Fig. 7 shows the changes in the spectrum slope of satellites launched at different times. It can be noted that the reflectance spectra of satellites with a shorter operating time have, in general, a greater spectrum slope than satellites launched at earlier dates, but this observational material does not allow us to draw an unambiguous conclusion about the relationship between this parameter and the operating time of the apparatus. Fig. 8 shows the change in the spectrum slope of the KazSat-1 satellite, currently uncontrolled.
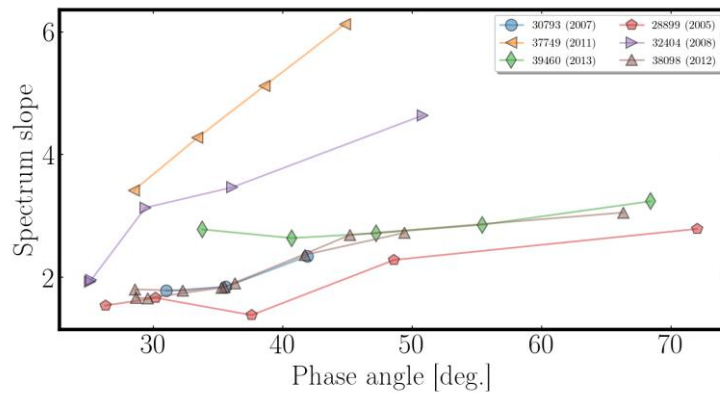

Fig. 7. Variation of the spectrum slope relative to the phase angle of the object.
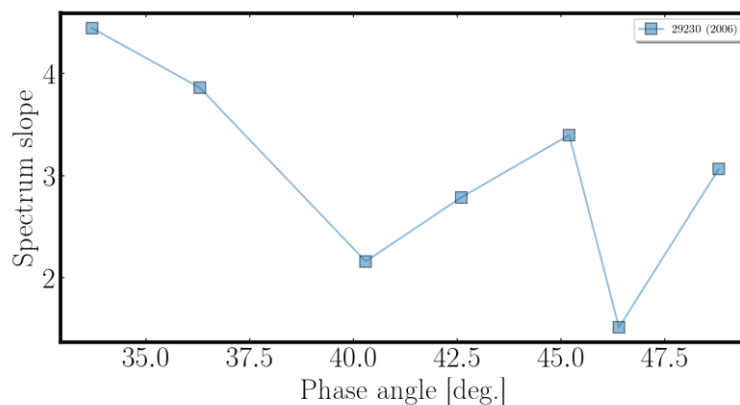

Fig. 8. The change in spectrum slope of KazSat-1 launched in 2006 and is currently uncontrolled.

Conclusion

The conducted studies have shown that the proposed method of observations and interpretation of the spectral data of the geostationary area is suitable for further research.

The analysis of the results also showed the need to obtain a large number of spectra for GSS of different configurations (geometry, platforms), for a wide range of phase angles, and different service life (after

orbital deployment). In addition, it is necessary to expand the studied spectral range into the infrared region of the spectrum. For future works, it is planned to conduct a comparative analysis of the obtained parameters of the reflection spectra of GSS with the parameters of the spectra of samples of materials and composites that are in the public domain. The preliminary result showed the possibility of obtaining the spectral characteristics of GSO, including uncontrolled spacecraft with rapidly changing illumination conditions (reflections) using an innovative spectrograph mounted on the AZT-20 telescope, which is planned to be fully operational in 2022 at the Assy-Turgen observatory.

REFERENCES

1 Alberto B., et. al. Physical characterization of the deep-space debris WT1190F: A testbed for advanced SSA techniques. *Advances in Space Research*, 2019, Vol. 63, pp. 371–393.

2 Reyes J.A., et. al. Spectroscopic behavior of various materials in a GEO simulated environment. *Acta Astronautica*, 2021, Vol. 189, pp. 576-583, doi: https://doi.org/10.1016/j.actaastro.2021.09.014

3 Bengtson M., et. al. Optical Characterization of Commonly Used Thermal Control Paints in a Simulated GEO Environment. *The Advanced Maui Optical and Space Surveillance Technologies Conference*, 2018, Proceedings, Hawaii, id.33.

4 Bedard M.D., Levesque M., Wallace B. Measurement of the photometric and spectral BRDF of small Canadian satellites in a controlled environment. *DRDC-VALCARTIER-SL*, 2011, Vol. 343, No 7, pp. 2011.

5 Cowardin H. et al. Observations of Titan IIIC Transtage fragmentation debris. *Proceedings of the Advanced Maui Optical and Space Surveillance Technologies Conference,* 2013, doi: https://amostech.com/2013-technical-papers/

6 NASA JSC Spacecraft Materials Spectral Database. 2018. Available at: https://ntrs.nasa.gov/ (Dec 10, 2021).

7 Farnham T.L., Schleiche D.G., A'Hearnc M.F. The HB Narrowband Comet Filters: Standard Stars and Calibrations. *Icarus*, 2000, Vol. 147, pp. 180–204. doi: https://doi.org/10.1006/icar.2000.6420.

8 Tedesco E.F., Tholen D.J., Zellner B. The eight-color asteroid survey - Standard stars. *Astronomy & Astrophysics*, 1982, Vol. 642, No A80, pp. 29.

9 Cayrel de Strobel G. *Stars resembling the Sun*. Available at https://doi.org/10.1007/s001590050006 (Jan 22, 2022)

10 Virtanen P., Gommers R., Oliphant T.E., et.al. SciPy 1.0: Fundamental Algorithms for Scientific Computing in Python. *Nature Methods*, 2022, Vol. 17, No 3, pp. 261-272.

11 Reyes J.A., Darren C. Characterization of Spacecraft Materials using Reflectance Spectroscopy. *The Advanced Maui Optical and Space Surveillance Technologies Conference Proceedings*, 2018, Hawaii, Ed.: S. Ryan, The Maui Economic Development Board, id.57.

12 Reyes J.A., et. al. Understanding optical changes in on-orbit spacecraft materials. *Proceedings of the SPIE*, 2019, Vol. 11127, id. 111270I, pp. 13, doi: 10.1117/12.2528926

13 Plis E.A., et. al. Solar panel coverglass degradation due to the simulated GEO environment exposure. *Proceedings of the SPIE*, 2021, Vol. 11727, id. 117270W, pp. 8. doi: 10.1117/12.2588655

14 Plis E.A., et. al. Effect of Simulated GEO Environment on the Properties of Solar Panel Coverglasses. *IEEE Transactions on Plasma Science*, 2021, Vol. 49, No 5, pp. 1679-1685. doi: 10.1109/TPS.2021.3070196

15 Fedorenko D.S., Legkov K.E., Modeling of the high-orbital satellite reflection spectrum. *T-Comm: Telecommunications and transport*, 2020, Vol. 14, No 11, pp. 14-20. doi: 10.36724/2072-8735-2020-14-11-14-20